

$O(N)$ and RP^{N-1} models in two dimensions

Martin Hasenbusch

DAMTP, Silver Street, Cambridge, CB3 9EW, England

(Received 7 September 1995)

I provide evidence that the 2D RP^{N-1} model for $N \geq 3$ is equivalent to the $O(N)$ -invariant nonlinear σ model in the continuum limit. To this end, I mainly study particular versions of the models, to be called constraint models. I prove that the constraint RP^{N-1} and $O(N)$ models are equivalent for sufficiently weak coupling. Numerical results for the step-scaling function of the running coupling $\bar{g}^2 = m(L)L$ are presented. The data confirm that the constraint $O(N)$ model is in the same universality class as the $O(N)$ model with standard action. I show that in the weak coupling limit periodic boundary conditions for the RP^{N-1} model correspond to fluctuating boundary conditions for the $O(N)$ model. The effect of boundary conditions on finite size scaling curves is discussed. It is concluded, in contrast with Caracciolo *et al.*, that RP^{N-1} and $O(N)$ models share a unique universality class.

PACS number(s): 11.15.Ha, 05.50.+q, 11.10.Lm, 64.60.Fr

I. INTRODUCTION

Motivated by the close analogy with non-Abelian lattice gauge theories in four dimensions nonlinear σ models in two dimensions have been studied intensively during the last 20 years. Most important both types of models were found to be asymptotically free [1].

Starting from the early 1980's so-called RP^{N-1} models were discussed. The spins of these models are elements of the real projective space in N dimensions. This space can be thought of as a sphere S^{N-1} where opposite points are identified. Hence in perturbation theory the RP^{N-1} model is equivalent with the $O(N)$ -invariant σ model. The fact however that the real projective space is not simply connected gives rise to topological defect structures similar to vortices in the two-dimensional (2D) XY model. The questions discussed in the literature are whether these defects induce a phase transition at a finite coupling or whether these nonperturbative effects survive in the weak coupling limit.

The lattice action of the RP^{N-1} model mostly discussed is

$$S = -\beta \sum_{\langle xy \rangle} (\vec{s}_x \vec{s}_y)^2, \quad (1)$$

where $\langle xy \rangle$ is a pair of nearest neighbor points on the lattice and \vec{s} is a unit vector in R^N . An alternative way to identify $-\vec{s}_x$ and \vec{s}_x is to introduce a Z_2 gauge field

$$S = -\beta \sum_{\langle xy \rangle} z_{\langle xy \rangle} \vec{s}_x \vec{s}_y, \quad (2)$$

where z takes the values 1 or -1 .

Similar models have been introduced to describe orientational phase transitions in nematic liquid crystals [2]. These models have mainly been studied in three dimensions, where a weak first-order phase transition is found (see [3] and references given in [4]).

The numerical study of RP^{N-1} models in 2D gave rise to much controversy. Some authors [5–7] find that their results are consistent with a phase transition at a finite coupling, while others doubt the existence of a phase transition but still see strong crossover effects between the strong and the weak coupling regime [3,8,4].

Recently Caracciolo *et al.* [9–11] argued that there is no phase transition in the RP^{N-1} models. They claimed, based on a finite size scaling analysis, that the RP^{N-1} models however have a weak coupling limit distinct from that of the $O(N)$ -invariant σ models. They claim even further that a whole sequence of universality classes can be obtained from mixed models.

In the following I will give evidence that rules out the scenario presented in [9–11]. For a particular type of the action of the $O(N)$ and the RP^{N-1} model I will show that the models are exactly equivalent for sufficiently small coupling. I discuss the scaling properties of vortices of the RP^{N-1} model with standard action in the weak coupling regime. I give numerical results for the step-scaling function introduced in [13] that supports that the constraint model gives the same universal results as the standard action. I show that the differences in the finite size scaling curves for the RP^2 and the $O(3)$ model found in [10,11] can be partially explained as a boundary effect.

II. THE CONSTRAINT $O(N)$ AND RP^{N-1} MODELS

Let me first define the models. The field variable \vec{s}_x is in both cases a unit vector in R^N . In the case of the $O(N)$ -invariant model the Boltzmann weight of a configuration is equal to 1 if

$$\vec{s}_x \vec{s}_y > C \quad (3)$$

for all nearest neighbor pairs of sites $\langle xy \rangle$ or else the Boltzmann weight is equal to 0. In [12] Seiler and Patrascioiu discuss the relation of the constraint $O(N)$ -invariant model with a particular percolation problem. Based on this percolation problem they argue that for sufficiently large C the constraint $O(N)$ -invariant model in two dimensions becomes massless. However it should be noted that they do not provide a proof for this scenario. In the following, in particular in Sec. IV, I assume that the constraint $O(N)$ -invariant model, analogous to the standard $O(N)$ -invariant lattice model at finite β , is massive for all $C < 1$.

In the case of the RP^{N-1} model $-\vec{s}_x$ and \vec{s}_x are identified and the constraint on the field configuration is given by

$$|\vec{s}_x \vec{s}_y| > C \quad (4)$$

for all nearest neighbors $\langle xy \rangle$. Equivalently one might introduce a gauge field $z_{\langle xy \rangle}$ taking the values -1 or 1 :

$$z_{\langle xy \rangle} \vec{s}_x \vec{s}_y > C. \quad (5)$$

In the following I shall show that the constraint $O(N)$ -invariant model and the constraint RP^{N-1} model are equivalent for $C > \cos(\pi/4)$. Let us consider a lattice where all closed paths are contractible; i.e., all closed paths can be shrunk to an elementary plaquette by removing single plaquettes sequentially. A hypercubical square lattice with open boundary conditions is an example for such a lattice.

Consider the class of 2^V , where V is the number of lattice points, configurations that arise from a given configuration \vec{s}_x by taking either $+\vec{s}_x$ or $-\vec{s}_x$ at each lattice point. Since

$$|\vec{s}_x \vec{s}_y| = |(-\vec{s}_x) \vec{s}_y| = |\vec{s}_x (-\vec{s}_y)| = |(-\vec{s}_x)(-\vec{s}_y)| \quad (6)$$

all configurations in such a class are either allowed or forbidden RP^{N-1} configurations. Obviously a class of configurations that is forbidden under the RP^{N-1} constraint contains no configuration that is allowed under the $O(N)$ constraint (with the same C). In the following I will demonstrate that for $C > \cos(\pi/4)$ a class of configurations that is allowed under the RP^{N-1} constraint contains exactly two configurations allowed under the $O(N)$ constraint, and therefore the partition functions are equal up to a trivial factor 2^{V-1} .

Take one configuration out of an allowed class of RP^{N-1} configurations. Pick one site x . Replace the spins on the other sites by

$$\vec{s}'_y = \vec{s}_y \prod_{\langle uv \rangle \in \text{path}(x,y)} \text{sgn}(\vec{s}_u \vec{s}_v). \quad (7)$$

The result of this construction is independent of the paths chosen if

$$\prod_{\langle uv \rangle \in \text{closed path}} \text{sgn}(\vec{s}_u \vec{s}_v) = 1 \quad (8)$$

for all closed paths on the lattice. For elementary loops consisting of four lattice points this is the case for $C > \cos(\pi/4)$. All other paths can be successively built up out of elementary loops, since we have chosen a simply connected lattice topology. When adding an elementary loop the sign of a loop is conserved since the sign of the product of the new links in the path is the same as for the old links. Hence the sign of any closed path is 1 for $C > \cos(\pi/4)$.

By construction $\text{sgn}(\vec{s}'_x \vec{s}'_y) = 1$ for all nearest neighbor pairs $\langle xy \rangle$. The second allowed $O(N)$ configuration within a class of allowed RP^{N-1} configurations is given by $\vec{s}''_x = -\vec{s}'_x$.

The idea behind this proof has been discussed for an action similar to that in Eq. (2) by Caselle and Gliozzi [6]. However for that action the rigorous proof for a pure gauge in the weak coupling limit is missing.

In Monte Carlo simulations one typically uses periodic boundary conditions, which leads to the lattice topology of a torus. Here loops exist that wind around the torus and hence cannot be contracted to an elementary loop.

In order to avoid classes of allowed RP^{N-1} configurations that contain no allowed $O(N)$ configurations one has to require $C > \cos(\pi/L)$ where L is the extension of the lattice in units of the lattice spacing. It is important to note that such boundary effects might well survive the continuum limit in a finite size scaling analysis. However this boundary effect can be reproduced by proper boundary conditions imposed upon the $O(N)$ model. For $C > \cos(\pi/4)$ a constraint RP^{N-1} model on a periodic lattice is equivalent to a constraint $O(N)$ model with fluctuating boundary conditions. Fluctuating boundary conditions mean that in the partition function one sums over periodic as well as antiperiodic boundary conditions. In the case of antiperiodic boundary conditions one identifies $\vec{s}(0,y) = -\vec{s}(L,y)$, $\vec{s}(L+1,y) = -\vec{s}(1,y)$, $\vec{s}(x,0) = -\vec{s}(x,L)$, and $\vec{s}(x,L+1) = -\vec{s}(x,1)$.

III. SCALING OF THE VORTEX DENSITY FOR THE STANDARD ACTIONS

For the standard actions of the RP^{N-1} model similar arguments apply. In the limit $\beta \rightarrow \infty$ the energy of a vortex should win against the entropy and vortices should play no role in the continuum limit of the theory.

Let us identify a frustrated plaquette in Eq. (2) with the center of a vortex. The classical solution of the \vec{s} field for a fixed gauge field with two frustrated plaquettes has an energy proportional to $\ln r$ where r is the distance in between these two frustrated plaquettes. Hence one can find a finite r_0 such that the energy is larger than $2/b_0$, where b_0 is the leading coefficient in the perturbative β function. Therefore the density of vortex pairs with a distance larger than r_0 dies out faster than the square of the inverse correlation length. Hence they should not play a role in the continuum limit of the theory.

IV. NUMERICAL RESULTS FOR THE CONSTRAINT MODELS

In this section I show that the constraint $O(N)$ model reproduces universal results of the $O(N)$ -invariant σ model. Therefore I compute the step-scaling function of Ref. [13] for three different values of the running coupling and compare the result with that of Ref. [13] obtained with the standard action. Furthermore I estimate the correlation length at $C = \cos(\pi/4)$ using the running coupling and also measure the correlation length for both the $O(N)$ and the RP^{N-1} model for $C < \cos(\pi/4)$ to check the importance of defects in the generation of the mass in the RP^{N-1} case.

The running coupling of [13] is defined by

$$\bar{g}^2 = \frac{2}{N-1} m(L)L, \quad (9)$$

where $m(L)$ is the mass gap on a lattice with extension L in spatial direction. The β function for the running coupling \bar{g}^2 is given by [13]

$$\beta(g^2) = -\frac{N-2}{2\pi} \bar{g}^4 - \frac{N-2}{(2\pi)^2} \bar{g}^6 - \frac{(N-1)(N-2)}{(2\pi)^3} \bar{g}^8 \dots \quad (10)$$

TABLE I. The renormalized coupling \bar{g}^2 from the constraint O(3) model. C gives the value of the constraint. L/a and L'/a are the lattice extensions in spatial direction.

C	L/a	L'/a	$\bar{g}^2(L)$	$\bar{g}^2(L')$
0.0515	4	8	1.0595(2)	1.2623(3)
0.0820	5	10	1.0595(2)	1.2564(3)
0.1047	6	12	1.0595(2)	1.2542(3)
0.1225	7	14	1.0595(2)	1.2540(2)
0.1371	8	16	1.0595(2)	1.2542(4)
0.1607	10	20	1.0595(2)	1.2545(3)
0.1786	12	24	1.0595(2)	1.2542(4)
0.2058	16	32	1.0595(2)	1.2559(3)
0.2255	20	40	1.0595(2)	1.2569(3)
0.2637	32	64	1.0595(2)	1.2582(6)
0.1992	4	8	0.8166(2)	0.9358(3)
0.2413	6	12	0.8166(2)	0.9234(2)
0.2663	8	16	0.8166(2)	0.9186(3)
0.2835	10	20	0.8166(2)	0.9171(2)
0.2967	12	24	0.8166(2)	0.9167(3)
0.2538	4	8	0.7383(2)	0.8373(2)
0.2924	6	12	0.7383(2)	0.8246(2)
0.3147	8	16	0.7383(2)	0.8197(3)
0.3299	10	20	0.7383(2)	0.8191(4)
0.3416	12	24	0.7383(2)	0.8174(3)
0.55	16	32	0.4491(2)	0.4759(4)
$1/\sqrt{2}$	16	32	0.2654(1)	0.2746(1)

The step-scaling function $\sigma(s, u)$ is the discrete version of the β function. It gives the value of the coupling after change of L by a factor of s starting from a coupling u .

The simulation was done using the evident modification of the single cluster algorithm [14]. A bond $\langle xy \rangle$ is called deleted if after the reflection of one of the spins \vec{s}_x or \vec{s}_y the constraint $\vec{s}_x \cdot \vec{s}_y > C$ is still satisfied.

A proof of ergodicity is given in the Appendix. The simulation results listed in Table I are based on about 10^7 single cluster updates. The correlation function was measured using the cluster-improved estimator [16]. The mass was extracted from the correlation function at distance L and $2L$.

Fitting the data of Table I to an ansatz

$$\Sigma(2, u, a/L) = \sigma(2, u) + c(a/L)^2. \quad (11)$$

I obtain $\sigma(2, 1.0595) = 1.2589(10)$ from $L/a \geq 16$, $\sigma(2, 0.8166) = 0.9150(8)$ from $L/a \geq 8$, and $\sigma(2, 0.7383) = 0.8159(8)$ from $L/a \geq 8$. These results can be compared with the step-scaling function obtained in [13] $\sigma(2, 1.0595) = 1.2641(20)$, $\sigma(2, 0.8166) = 0.9176(8)$, and $\sigma(2, 0.7383) = 0.8166(9)$. The slight disagreement (about 2 standard deviations) might well be explained by deviations of the corrections to finite size scaling from the fit ansatz chosen.

The exact prediction for the mass gap given by [15]

$$\frac{m}{\Lambda_{\overline{\text{MS}}}} = \frac{8}{e}, \quad (12)$$

TABLE II. The second moment correlation length in the vector (ξ_v) and tensor (ξ_t) channel for the constraint O(3)-invariant vector model for various values of the constraint C .

C	L	ξ_v	ξ_t
0.00	64	11.20(5)	3.29(6)
0.10	128	23.3(2)	6.9(2)
0.2255	400	76.7(4)	24.0(6)

where $\overline{\text{MS}}$ denotes the modified minimal subtraction scheme, for $N=3$ and the conversion factor for the Λ parameters

$$\Lambda = \frac{e^{-\Gamma'(1)}}{4\pi} \Lambda_{\overline{\text{MS}}} \quad (13)$$

given in [13] allows us to give an estimate for the infinite volume correlation length based on the measurement of the correlation length on a finite lattice. Taking the Monte Carlo result for the running coupling given in Table I I obtain $\xi = 0.7 \times 10^5$ as estimate for the correlation length at $C=0.55$ and $\xi = 0.6 \times 10^9$ as estimate at $C = \cos(\pi/4)$, where the O(3) and RP² constraint models become identical.

In addition I performed some simulations for both the constraint O(N) model and the constraint RP^{N-1} model at smaller C values such that the correlation length ξ is much smaller than the lattice size L . Here I adopted the definitions used in [9–11].

The correlation function in the vector channel is defined by

$$G_v(x, y) = \langle \vec{s}_x \cdot \vec{s}_y \rangle. \quad (14)$$

Since naively this quantity vanishes identically under the symmetries of the RP^{N-1} model one considers the tensor channel with the correlation function

$$G_t(x, y) = \langle (\vec{s}_x \cdot \vec{s}_y)^2 \rangle - \frac{1}{N}. \quad (15)$$

Starting from these definitions of the correlation function one obtains the susceptibility

$$\chi = \frac{1}{V} \sum_{x, y} G(x, y) \quad (16)$$

and

$$F = \frac{1}{V} \sum_{x, y} \cos\left(\frac{2\pi}{L} k(x-y)\right) G(x, y) \quad (17)$$

with $k = (1, 0)$ or $k = (0, 1)$.

The second moment correlation length is now defined as

$$\xi = \frac{\sqrt{\chi/F - 1}}{2 \sin(\pi/L)}. \quad (18)$$

In Table II some results for the constraint O(3) model are given. It is remarkable that already for $C=0$ the correlation length is larger than ten. The ratio of the correlation length in the vector and the tensor channel is about $\xi_v/\xi_t = 3.3(1)$.

In Table III my results for the constraint RP² model are summarized. At $C=0.55$ there is a factor of about 10^3 in between the correlation lengths of the O(3) and the RP²

TABLE III. The second moment correlation length in the tensor channel ξ_t for the constraint RP^2 model for various values of the constraint C .

C	L	ξ_t
0.50	64	4.72(2)
0.51	64	5.66(2)
0.52	128	7.10(6)
0.53	128	9.06(5)
0.55	128	16.52(7)

model. This means that it is practically impossible to see the true asymptotic behavior of the constraint RP^2 model in a computer simulation.

V. FINITE SIZE SCALING AND UNIVERSALITY

In this section I shall demonstrate that the difference in the finite size scaling curves observed in [9,10] can be explained in part by the boundary effect discussed above. I simulated the $O(3)$ -invariant model with the standard action on a square lattice using fluctuating boundary conditions in both lattice directions. For the updates of the boundary conditions I used the boundary flip algorithm proposed in [17] for the Ising model and generalized to $O(N)$ vector models in [18].

Most of the runs I performed at $\beta=1.4$, $\beta=1.5$, and $\beta=1.6$. The true correlation lengths for these β values are $\xi=6.90(1)$, $\xi=11.09(2)$, and $\xi=19.07(6)$, respectively [16]. I used lattice sizes ranging from $L=6$ to $L=128$. Throughout I performed 100 000 measurements. I performed a measurement after one boundary-flip update for each direction and roughly *cluster-size over lattice-size* standard single cluster updates. In Fig. 1 the dimensionless quantity $\chi_t(2L)/\chi_t(L)$ is plotted as a function of ξ/L , where ξ is the infinite volume correlation length. I give the results for fluctuating boundary conditions (circles) and for comparison the

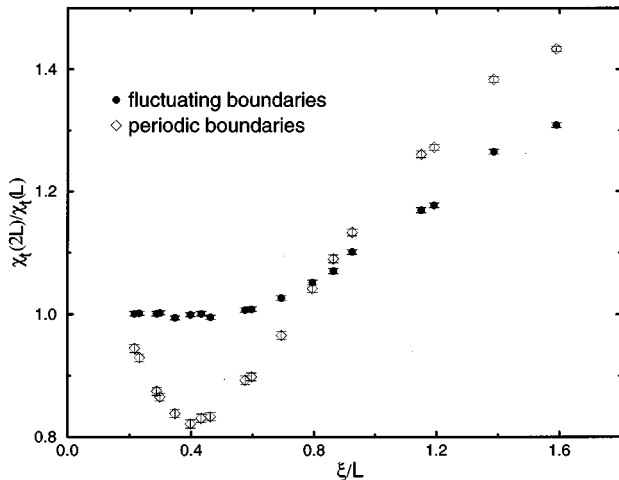


FIG. 1. The dimensionless quantity $\chi_t(2L)/\chi_t(L)$ is given as a function of $\xi_v(L=\infty)/L$ for the $O(3)$ model. The data for ξ_v are taken from [16]. The data points with the circles are obtained with fluctuation boundary conditions while those with diamonds are obtained with periodic boundary conditions.

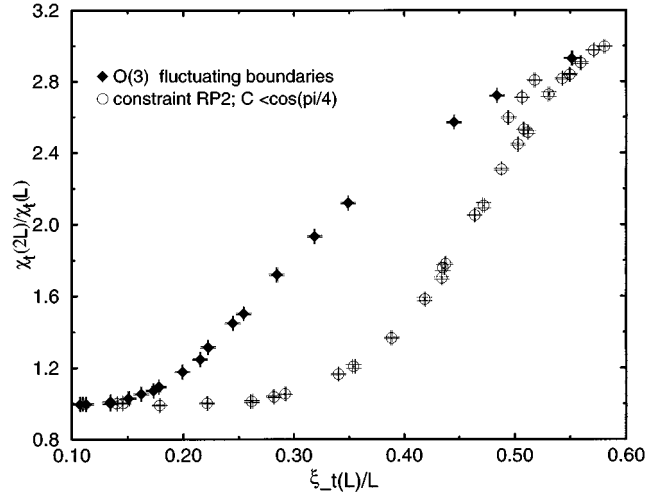


FIG. 2. $\chi_t(2L)/\chi_t(L)$ is plotted as a function of $L/\xi_t(L)$ for the constraint RP^2 model as well as the $O(3)$ model with fluctuating boundary conditions. In the case of the constraint RP^2 model data for $C=0.5, 0.51, 0.52, 0.53, 0.55, 0.56, 0.57$, and 0.59 and $L=8$ up to $L=128$ are shown. The β values for $O(3)$ range from 1.4 to 3.4. For most of the data points $L=16$ is used.

results with periodic boundary conditions (diamonds). Comparing with Fig. 2 of [11] one has to note that Caracciolo *et al.* use $L/\xi_t(L)$ as parameter on the x axis. My result for periodic boundary conditions is consistent with that given in Fig. 2(b) of [11]. The fluctuating boundary conditions remove the characteristic dip visible in the finite size scaling curve for periodic boundary conditions. The finite size scaling curve for fluctuating boundary conditions looks qualitatively much like that of Fig. 2(a) of [11] (RP^2 -like models).

However a quantitative comparison, taking into account the different parameters for the x axis, reveals that the difference between the finite size scaling curve of the RP^2 model presented in Fig. 2(a) of [11] and that of the $O(3)$ model is not fully explained by the boundary effect discussed above. This fact has to be explained by the presence of vortices at the finite β values of the data given in Fig. 2(a) of [11].

In this context it is illuminating to compare the finite size scaling curve of the constraint RP^2 model for $C < \cos(\pi/4)$ with that of the $O(3)$ model with fluctuating boundary conditions. In Fig. 2 $\chi_t(2L)/\chi_t(L)$ is plotted as a function of $L/\xi_t(L)$ for the constraint RP^2 model as well as the standard $O(3)$ model with fluctuating boundary conditions. In the case of the constraint RP^2 model data for $C=0.5, 0.51, 0.52, 0.53, 0.55, 0.56, 0.57$, and 0.59 and $L=8$ up to $L=128$ are shown. The β values for $O(3)$ range from 1.4 to 3.4. For most of the data points $L=16$ is used.

The two curves are clearly distinct, and the RP^2 data for different C values fall rather nicely onto a unique curve. Furthermore the curve produced by the constraint RP^2 data is quite similar to that obtained from the action given by Eq. (1) [20]. However we should keep in mind the proof of Sec. II.

In the following section an attempt is made to explain this puzzling observation.

VI. IS THERE A PHASE TRANSITION?

In order to understand the phase structure of the RP^{N-1} models one might, in analogy with the Kosterlitz-Thouless (KT) scenario of the XY model [19], discuss the renormalization-group (RG) flow of the models in a two-dimensional parameter space. In addition to the coupling g^2 one might introduce a coupling parameter μ for the plaquette-term, controlling the density of vortices:

$$S = -\frac{1}{g^2} \sum_{\langle xy \rangle} z_{xy} \vec{s}_x \cdot \vec{s}_y + \ln \mu \sum_p z_p, \quad (19)$$

where $z_p = \prod_{\langle xy \rangle \in p} z_{xy}$.

I will make no attempt here to derive the RG flow equations. However certain qualitative features and their consequences seem to be evident: (a) For $(g^2, 0)$ the standard β function of the O(N) model is recovered; (b) vortices cause disorder. Therefore a nonvanishing μ should amount to a positive contribution in the derivative of g^2 with respect to the logarithm of the cutoff scale and hence accelerate the flow towards strong coupling.

Statement (a) rules out that a possible phase transition in the RP^{N-1} model is KT like, since the fixed point of the KT transition is purely Gaussian. Furthermore statement (b) rules out any fixed point that might occur at a finite μ .

Still we have to explain why Monte Carlo simulations and strong coupling expansions seem to be in favor of a phase transition. It seems plausible that in analogy with the KT-flow equations μ is irrelevant for small coupling g^2 but becomes relevant above some threshold value g_t^2 . That means above g_t^2 the RG trajectories are driven off from the renormalized trajectory of the O(N)-invariant model.

VII. CONCLUSIONS

I have proven that the constraint O(N) and constraint RP^{N-1} model become equivalent for $C > \cos(\pi/4)$. Using the renormalized coupling $\tilde{g}^2 = m(L)L$ I estimated the correlation length at $C = \cos(\pi/4)$ to be about $\xi = 0.6 \times 10^9$ for both models with $N=3$. For C values being smaller, such that $\xi \ll 1000$, the models display huge differences. This means that the asymptotic behavior of the constraint RP² model practically cannot be observed in a computer simulation. I argue that a similar scenario holds for models with a standard action. As $\beta \rightarrow \infty$ vortices in the RP^{N-1} model should vanish and the RP^{N-1} becomes equivalent to an O(N) model by the virtue of a gauge fixing.

On lattices with periodic boundary conditions one has to notice that paths winding around the lattice are not contractible. The effect of such loops in the RP^{N-1} model amount to fluctuating boundary conditions in the equivalent O(N) model. I demonstrated numerically that this fact partially explains the differences found in the finite size scaling curves for the O(3) and RP² models observed in [10,11].

Note added. My conclusions are confirmed by work of Niedermayer, Weisz, and Shin [21], which came to my knowledge after the present work was finished.

ACKNOWLEDGMENTS

I would like to thank M. Caselle, I. T. Drummond, R. R. Horgan, and K. Pinn for discussions. This work was supported by the Leverhulme Trust under Grant No. 16634-AOZ-R8 and by PPARC.

APPENDIX

In the following I prove that the single cluster algorithm applied to the constraint O(N)-invariant model is ergodic.

It is sufficient to show that any allowed configuration can be transformed in a finite number of cluster-update steps to the configuration $\vec{s} = (1, 0, \dots, 0)$ for all sites.

Let us consider an $N=2$ (XY) model with a bond dependent constraint $C_{\langle xy \rangle}$. Assume that the spins are distributed in an angle range $[0, \alpha_k]$ with respect to the 1 axis. (The largest range to start with is $[0, 2\pi]$.)

Take a reflection axis which has an angle $\alpha_k/2$ with the 1 axis. Per construction none of the sites x with $\phi_x > \alpha_k/2$ is connected via a frozen bond with a site y with $\phi_y < \alpha_k/2$. Hence all spins can be moved into the range $[0, \alpha_k + 1]$ with $\alpha_{k+1} = \alpha_k/2$ using a finite number (smaller or equal the number of sites) of cluster updates. Iterating this process, in a finite number of steps all spins can be put into the range $[0, \min \text{arc cos}(C_{\langle xy \rangle})]$. Now take for each site a reflection axis with $\alpha_x = \phi_x/2$. Per construction all these clusters are single site clusters.

We hence constructed a sequence of a finite number of cluster updates that transforms an arbitrary configuration to the $s = (1, 0)$ for all sites configuration.

For general N this procedure can be iterated. Consider the N th and $(N-1)$ th component as an embedded XY model. Remove the N th component. Go ahead until $s = (1, 0, \dots, 0)$ for all sites is reached.

-
- [1] A.M. Polyakov, Phys. Lett. **59B**, 79 (1975); E. Brezin and J. Zinn-Justin, Phys. Rev. Lett. **36**, 691 (1976); Phys. Rev. B **14**, 3110 (1976).
- [2] P.A. Lebowitz and G. Lasher, Phys. Rev. A **6**, 426 (1972).
- [3] S. Duane and M.B. Green, Phys. Lett. **103B**, 359 (1981).
- [4] C. Chiccoli, P. Pasini, and C. Zannoni, Physica A **148**, 298 (1988).
- [5] S. Solomon, Phys. Lett. **100B**, 492 (1981).
- [6] M. Caselle and F. Gliozzi, Phys. Lett. **147B**, 132 (1984).
- [7] H. Kunz and G. Zumbach, Phys. Lett. B **257**, 299 (1991); Phys. Rev. B **46**, 662 (1992).
- [8] S. Solomon, Y. Stavans, and E. Domany, Phys. Lett. **112B**, 373 (1981).
- [9] S. Caracciolo, R.G. Edwards, A. Pelissetto, and A.D. Sokal, in *Lattice '92*, Proceedings of the International Symposium, Amsterdam, The Netherlands, 1992, edited by J. Smit and P. van Baal [Nucl. Phys. B (Proc. Suppl.) **30**, 815 (1993)].
- [10] S. Caracciolo, R.G. Edwards, A. Pelissetto, and A.D. Sokal,

- Phys. Rev. Lett. **71**, 3906 (1993).
- [11] S. Caracciolo, R.G. Edwards, A. Pelissetto, and A.D. Sokal, in *Lattice '93*, Proceedings of the International Symposium, Dallas, Texas, edited by T. Draper *et al.* [Nucl. Phys. B (Proc. Suppl.) **34**, 129 (1994)].
- [12] E. Seiler and A. Patrascioiu, in *Lattice '92* [9], p. 184.
- [13] M. Lüscher, P. Weisz, and U. Wolff, Nucl. Phys. **B359**, 221 (1991).
- [14] U. Wolff, Phys. Rev. Lett. **62**, 361 (1989) .
- [15] P. Hasenfratz, M. Maggiore, and F. Niedermayer, Phys. Lett. B **245**, 522 (1990).
- [16] U. Wolff, Nucl. Phys. **B334**, 581 (1990) .
- [17] M. Hasenbusch, Physica A **197**, 423 (1993).
- [18] A.P. Gottlob and M. Hasenbusch, J. Stat. Phys. **77**, 919 (1994).
- [19] See, for example, J.M. Kosterlitz and D.J. Thouless, J. Phys. C **6**, 1181 (1973); J.M. Kosterlitz, *ibid.* **7**, 1046 (1974); J.V. José, L.P. Kadanoff, S. Kirkpatrick, and D.R. Nelson, Phys. Rev. B **16**, 1217 (1977).
- [20] A. Sokal (private communication).
- [21] F. Niedermayer, P. Weisz, and D.-S. Shin, Phys. Rev. D (to be published).